Nonuniversal Velocity Fluctuations of Sedimenting Particles

Shang-You Tee,[1,2] P. J. Mucha,[3] Luca Cipelletti,[1,2,*] S. Manley,[1,2] M. P. Brenner,[2] P. N. Segre,[1,2,†] and D. A. Weitz[1,2]

[1]*Department of Physics, Harvard University, Cambridge, Massachusetts 02138*
[2]*Division of Engineering and Applied Sciences, Harvard University, Cambridge, Massachusetts 02138*
[3]*School of Mathematics, Georgia Institute of Technology, Atlanta, Georgia 30332*
(Received 2 January 2002; published 15 July 2002)

Velocity fluctuations in sedimentation are studied to investigate the origin of a hypothesized universal scale [P. N. Segre, E. Herbolzheimer, and P. M. Chaikin, Phys. Rev. Lett. **79**, 2574 (1997)]. Our experiments show that fluctuations decay continuously in time for sufficiently thick cells, never reaching steady state. Simulations and scaling arguments suggest that the decay arises from increasing vertical stratification of particle concentration due to spreading of the sediment front. The results suggest that the velocity fluctuations in sedimentation depend sensitively on cell geometry.

The slow sedimentation of a dilute suspension of particles through a viscous fluid is an important and fundamental problem in fluid mechanics, impacting processes ranging from formation of geological deposits to removal of contaminants in ground water to centrifugation of proteins. Despite its apparent simplicity, the complexities of hydrodynamic interactions between the particles have provoked a long-standing controversy and sedimentation is still intensely debated to this day [1,2]. A single spherical falling particle falls at the well-known Stokes velocity $v_s = (2/9)a^2 \Delta \rho g / \eta$, where a is the particle radius, $\Delta \rho$ is the density difference, g is the gravitational constant, and η is the dynamic viscosity. A uniform concentration of particles sediments more slowly than a single particle because of the confinement of the suspension within the finite cell: fluid must rise as particles sink, and this backflow slows the sedimentation. Remarkably, the average particle velocity is universal, independent of the cell size and shape [3]. However, the long-range interparticle hydrodynamic interactions drive considerable fluctuations of the velocity about its mean. Simple arguments and simulations [4] suggest that the magnitude of the velocity fluctuations should diverge with system size. By contrast, experiments [5] conclude that the fluctuations are independent of the system size; indeed recent experiments [1,6] even argue that they are universal, organized into swirls of characteristic size $\xi \sim 15a\phi^{-1/3}$, for solid volume fraction ϕ, with characteristic velocity fluctuations scaling like $\Delta v \sim \phi^{1/3}$. The simplicity of these experimental results is appealing; however, the origin of this scaling remains a mystery [7–9]. The behavior of velocity fluctuations must be resolved if sedimentation is to be understood in even the most rudimentary way.

An important key to understanding this problem is the dependence of the characteristic velocity fluctuations on cell thicknesses [8]. Virtually all experimental evidence is restricted to a narrow range of cell thickness [1,5,6]; thus, a careful investigation over an extended range of thicknesses is essential, both to critically test the universality and to help determine its underlying origin. In this Letter, we present experimental evidence suggesting that the magnitude of the initial fluctuations increases with cell size. However, for sufficiently thick cells the magnitude also decreases over the entire time of the experiment, so that a steady state does not exist.

To help understand these surprising results, we perform numerical simulations of up to 10^6 particles, which capture the experimentally observed behavior. This suggests that the decrease of the fluctuations is driven by the broadening of the front [10] separating the suspension from the particle-free fluid above it; the resulting stratification of the particle concentration suppresses large fluctuations. A simple scaling picture quantitatively predicts the magnitude and scale of the velocity fluctuations observed experimentally. The decay in the fluctuations makes it impossible to define a steady-state value except for the thin cells that have been predominantly studied to date [1]. This qualitatively changes the essential experimental observations which define this phenomenon.

We measure velocity fluctuations using particle image velocimetry (PIV). Monodisperse glass particles, of radius $a = 26.5 \pm 1.8$ μm and volume fraction $\phi = 0.001$–0.01, are index matched with a mixture of glycerol and water. The resulting viscosity is measured with a rheometer to range from $\eta = 10$–20 cP. These particles have high Peclet number (Pe $\approx 7 \times 10^6$) and low Reynolds number (Re $\approx 7 \times 10^{-4}$), so both Brownian diffusion and inertial effects are negligible. The cell depth, d, is varied between $30a \leq d \leq 500a$; the width, w, is always greater than d, while the height, h, is always considerably greater. To suppress temperature fluctuations across the sample, the cell is immersed in a stirred water bath at a temperature of $T = 22.0 \pm 0.1\,°C$. A CCD camera images a region of $\sim 1.3 \times 1.8$ cm^2, centered far from the cell bottom and the sediment front. The depth of focus of the lens ~ 0.5 cm so the signal samples particles across the entire cell cross section. Initial particle distributions are prepared by vigorously shaking the cell or by stirring with a rotating blade. We determine the vertical velocity fluctuations, $\Delta v = \langle (v - v_{\text{sed}})^2 \rangle^{1/2}$, where v is the local vertical

component, measured with PIV, and v_{sed} is the measured average velocity of the sedimentation front.

For thin cells, $d \leq 140a$, the fluctuations decay to a uniform value after an initial transient (solid squares, $\phi = 0.001$ and circles, $\phi = 0.01$ in Fig. 1), in accord with previous measurements [1]. We also observe spatially correlated swirls, similar in scale to previous measurements [Fig. 2(a)]. For thicker cells, with $d > 140a$, a completely unexpected behavior is observed. The magnitude of Δv decays through the entire experiment, never reaching a steady state (solid triangles, Fig. 1). We observe that whenever the initial $\Delta v \geq v_{\text{sed}}$, Δv decays in time.

Because these results are so unexpected, we use a completely different technique, ultrasmall angle dynamic light scattering (DLS) [11], to measure Δv in a different system. We use silica spheres, with $a = 1.5$ or 2.5 μm and with $0.018 < \phi < 0.087$, suspended in index-matching mixtures of glycerol and water or of benzyl and ethyl alcohol, with $\eta \approx 1$–30 cP; here $10^{-8} < \text{Re} < 10^{-5}$, and $7 < \text{Pe} < 50$. The temperature is controlled at $T = 22.0 \pm 0.1\,^{\circ}\text{C}$ and d is varied from $25a$ to $2300a$. The sample is stirred with a pipette as it is loaded into the cell. A CCD camera is used as a multispeckle detector; by simultaneously collecting data from a large number of independent speckles, each at the same scattering vector, q, we can measure the complete correlation function for several q in less than $200\tau_s$, enabling us to follow time dependent behavior. For $qs \geq 1$, where $s = a\phi^{-1/3}$ is the mean interparticle spacing, the correlation function is well described by $f(q, t) = \exp\{-(qt\Delta v/2)^2\}$ [12]. The dynamic light scattering ex-

periments exhibit the same behavior as the PIV experiments: For thick cells, with $d > 250a$, the initial value of Δv is greater than v_{sed}, and Δv decreases continuously through the whole run (hatched symbols, Fig. 1). For thin cells, Δv decays from an initial transient value but then remains constant throughout the whole run, with a value consistent with previous measurements. Thus, the light scattering results confirm the anomalous behavior seen with the PIV.

The data for Δv for thick cells show none of the universal behavior previously reported for thin cells; instead, the values of Δv are larger, with continuous decay over the whole run. This suggests a completely new form of scaling: We fit the data (after the inertial transients associated with sample preparation abate) to an exponential, $\Delta v(t) = \Delta v_0 \exp(-t/\tau)$; then the data are normalized by Δv_0, and the time by τ. As shown in Fig. 3(a), the scaled data all lie on a single master curve. The values of Δv_0 depend sensitively on initial mixing and show no discernible trend. However, τ clearly depends on h, as shown in Fig. 3(b), with $\tau \sim h^{1.2}$. There is no significant dependence of τ on either d or w.

To help understand these surprising results, we perform numerical simulations of a dilute-limit sedimenting suspension in a large aspect ratio cell with up to 4×10^6 particles. Hydrodynamic interactions between the point particles, sidewalls, and the appropriate backflow are all
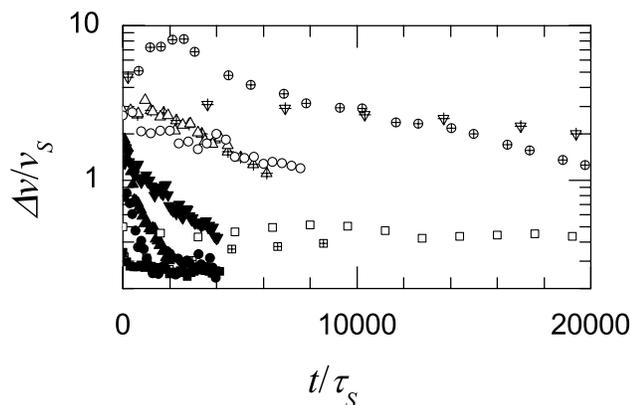

FIG. 1. Velocity fluctuations as a function of time (in units of $\tau_s = a/v_s$). Solid, hatched, and open symbols correspond to PIV, DLS, and simulations, respectively, for thick and thin cells of different heights. The velocity fluctuations decay as a function of time for thick cells and are constant for thin cells. The DLS data continue to decay (not shown) for the full experimental runs. Data are labeled by cell dimensions $(d/a \times w/a \times h/a)$ PIV: (square) $113 \times 1890 \times 11\,300$, (circle) $113 \times 1890 \times 11\,300$, (triangle) $226 \times 2260 \times 5280$, (inverted triangle) $226 \times 2260 \times 10\,600$; DLS: (square) $103 \times 1920 \times 19\,200$, (circle) $400 \times 7200 \times 28\,400$, (triangle) $660 \times 7200 \times 12\,000$, (inverted triangle) $1330 \times 16\,700 \times 45\,300$; simulations: (square) thin cell, (circle) thick cell, (triangle) thick cell.
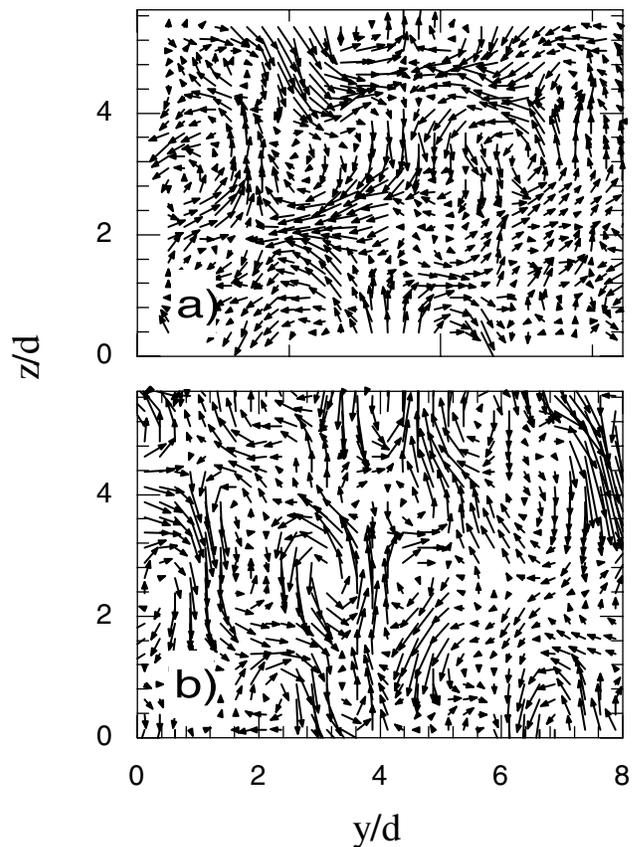

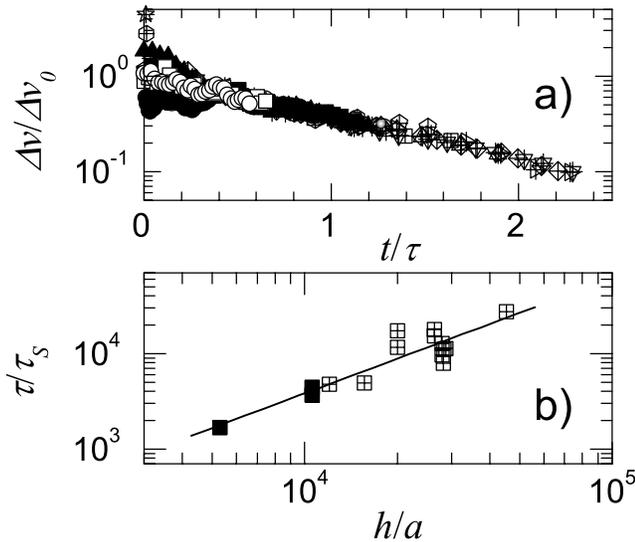FIG. 2. PIV velocity fields from (a) experiments and (b) numerical simulations in steady-state thin cells.

FIG. 3. (a) Master curve of the normalized velocity fluctuations $\Delta v(t)/v_s$ plotted as a function of time scaled by the characteristic relaxation time τ in thick cells. Open, solid, and hatched symbols are simulations, PIV, and DLS measurements, respectively. (b) Characteristic decay time, τ, of velocity fluctuations in thick cells, as a function of h. Solid and hatched symbols are PIV and DLS data, respectively. The solid line is a fit to a power law which yields an exponent of 1.21 ± 0.15.

included [13]. The simulations show stable velocity fluctuations when the computational cell is periodic in the height dimension, with the sizes of the fluctuations agreeing quantitatively with those predicted by assuming a Poisson distribution of particles across the gap. The simulations also correctly reproduce the spatial correlations of the velocity fluctuations observed in a thin cell, as shown in Fig. 2(b). No decay in Δv is observed even when polydispersity, a Boycott effect [14], or an imposed shear are introduced. However, as soon as a cell bottom and a sedimentation front are included, a decay is observed, provided $\Delta v > v_{\text{sed}}$; by contrast, when $\Delta v < v_{\text{sed}}$, as is the case for a thin cell, Δv remains roughly constant in time. Typical simulation results are shown in Fig. 1, for thin (open squares) and thick (open circles and triangles) cells; the decaying data also scale on the master curve in Fig. 3(a). Thus, these simulations correctly capture the essential experimental observations.

Why do the fluctuations decay? An examination of the simulations reveals that the spreading of the sediment front is pronounced when $\Delta v > v_{\text{sed}}$. This causes a stratification of the particle concentration that can extend to the imaging window, even when the window is located well below the front. This stratification evolves in time, owing to the broadening of the front.

Even a very small stratification [9] can substantially reduce Δv. Velocity fluctuations are driven by fluctuations in particle concentration, determined by Poisson statistics. A region of size ℓ has a typical concentration fluctuation of $\Delta\phi \approx \sqrt{\phi a^3/\ell^3}$; its velocity is determined by balancing its buoyant weight, $\Delta\phi\Delta\rho g\ell^3$, with its Stokes drag,

$6\pi\eta\ell\Delta v$, giving $\Delta v_\ell = Cv_s\sqrt{\phi\ell/a}$. The velocity fluctuations create an effective diffusivity, $D = \ell\Delta v$. In the absence of stratification, concentration fluctuations are produced and destroyed due to randomness on the same time scale, $\tau_D \approx \ell^2/D \approx \ell/\Delta v$; thus they are advected a distance ℓ in their lifetime. However, stratification leads to a change in the particle concentration, which limits how far down a heavy concentration fluctuation can fall or how far up a light one can float. Any concentration change greater than $\Delta\phi$ destroys the bouyancy mismatch, so the fluctuation cannot advect as far. For a locally linear decrease in ϕ with height, $\phi = \phi_0(1 - \beta z)$, the stratification causes the lifetime of a fluctuation to be limited to $\tau_S = L/\Delta v$, where $L = \Delta\phi/\beta\phi_0$ is the length scale over which stratification changes ϕ by $\Delta\phi$. Thus, stratification cuts off fluctuations when $\tau_S < \tau_D$ or $\ell > L$. The largest fluctuations are thus on a scale $\ell \sim a\phi_0^{-1/5}(\beta a)^{-2/5}$ with $\Delta v \sim v_s\phi_0^{2/5} \times (\beta a)^{-1/5}$. These arguments apply when the size of the fluctuation is smaller than the cell depth $\ell < d$; larger fluctuations are controlled by the small cell dimension, d. Setting $\ell \sim d$ yields the critical stratification: $\beta_{\text{crit}}d \sim 1/\sqrt{N_d}$, where N_d is the number of particles in a volume d^3. This decreases rapidly with increasing cell thickness. For our experiments, $\beta_{\text{crit}}d \sim 10^{-3}$; a stratification of 10^{-3} across a distance of order the cell depth is sufficient to cut off the velocity fluctuations.

The simulations suggest that the decay of the fluctuations results from the spreading of the sedimentation front, which causes β to *increase* with time. We quantify this with a simplified model for the sediment front, including the effects of particle diffusion (due to the hydrodynamic interactions) and settling [10]. The particle concentration approximately obeys $\partial_t\phi + v_{\text{sed}}\partial_z\phi = D\partial_z^2\phi$, where we use $D = Kdv_s\sqrt{\phi_0 d/a}$ with the prefactor K measured from our simulations. This model for D explicitly accounts for the dependence of the velocity fluctuations on the cell depth. This model determines the spreading of the sediment front, thereby giving $\beta(t)$ in the measurement window. This explains why the decay time of Δv depends on the cell height: When $\Delta v > v_{\text{sed}}$, the spreading of the sediment front occurs on the same time scale as its advection, which is of order h/v_{sed}. We note that all the volume fractions used in this work are sufficiently low that there are no ϕ-dependent effects influencing the sedimentation rate.

The key prediction of this model is the time evolution of the stratification of the particle concentration caused by the spreading of the sedimentation front. To confirm this prediction experimentally, we measure the particle concentration as a function of both time and cell height. We monitor the attenuation of the total transmitted light in the PIV experiments and use Beer's law to determine the varia-tion of ϕ as a function of z and time; typical results are shown in Figs. 4(a)–4(c). Initially, ϕ is relatively constant along the cell; however, the profile quickly stratifies. Identical behavior is obtained from the simulations, as shown in Figs. 4(d)–4(f). Strikingly, as shown by the
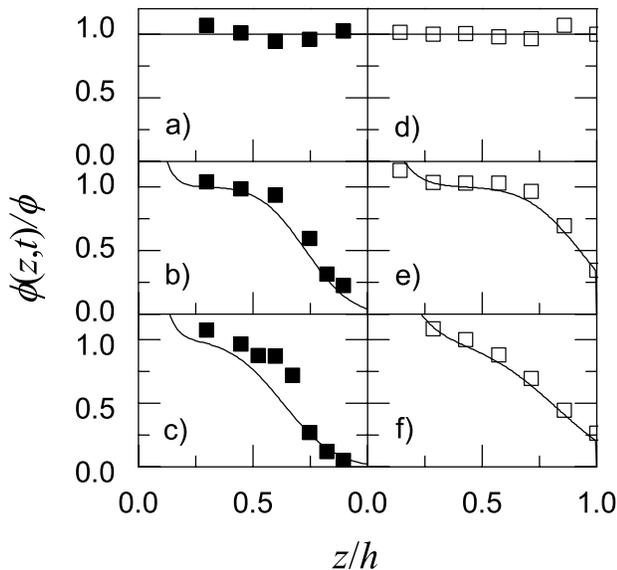
FIG. 4. Concentration (normalized by ϕ) profile versus reduced height, z/h, for different times, for PIV and simulation (at different operating conditions). Left panels are experimental data for reduced time, $t/\tau =$ (a) 0.00, (b) 0.27, and (c) 0.37 and right panels show simulation data for reduced time, $t/\tau =$ (d) 0.00, (e) 0.06, and (f) 0.17. Lines are advection-diffusion model 1D model using a Poisson model for the particle diffusivity.

solid lines through the data, our analytic model is in excellent accord with both experiment and simulation, using no adjustable parameters except for the diffusivity, which was determined from the simulations.

We remark that there is one important difference between the experiments and the simulations: the initial experimental mixing process certainly causes an initial stratification in addition to that produced by the spreading sediment front. Since β_{crit} is so tiny for thick cells, this can be quantitatively significant and likely causes the variation in Δv_0 in the experiments.

The results reported here suggest a picture for the velocity fluctuations in sedimentation that is quantitatively consistent with all previously reported results. When $\Delta v < v_{sed}$, the fluctuations are controlled by the cell depth until a critical stratification (controlled by the spreading sediment front) develops at the imaging window, after which the fluctuations decay. When $\Delta v > v_{sed}$, the spreading of the sediment front is greatly enhanced. We calculate that previous experiments [1] typically develop a stratification $\beta > \beta_{crit}$ well before the sediment front passes through the imaging window, suggesting that stratification is also playing an important role in these experiments [13]. Once the critical stratification is exceeded, the predicted ϕ dependencies of the velocity fluctuations, $\Delta v \sim \phi^{2/5}$, and the correlation length, $\ell \sim \phi^{-1/5}$, are, within experimental uncertainty, both in accord with the previous reports of $\Delta v \sim \phi^{1/3}$, and $\ell \sim \phi^{-1/3}$ [1]. Moreover, even the characteristic magnitude of the fluctuations is in accord with previously reported experiments: We

have $\ell \approx C_\xi a \phi^{-1/3}$, with $C_\xi = [\phi^{1/3}/(\beta a)]^{2/5}$, which has only a weak dependence on both ϕ and β; for $\phi = 10^{-2}$, $d/a \sim 10^2$, and $\beta \sim \beta_{crit}$, we obtain $C_\xi \approx 20$, in good accord with the previously measured value of ~ 15 [1].

The picture presented here suggests that the velocity fluctuations in sedimentation are not universal; rather, through a combination of the smallest cell dimension and local stratification, the velocity fluctuations depend on both cell geometry and experiment duration.

*Present address: GDPC cc 26, Universite Montpellier II, P.E. Bataillon, Montpellier 34000, France.
†Present address: NASA Marshall Space Flight Center, Huntsville, Alabama 35812.
[1] P. N. Segre, E. Herbolzheimer, and P. M. Chaikin, Phys. Rev. Lett. **79**, 2574 (1997).
[2] S. Ramaswamy, Adv. Phys. **50**, 297 (2001).
[3] G. K. Batchelor, J. Fluid Mech. **52**, 245 (1972).
[4] R. E. Caflisch and J. H. C. Luke, Phys. Fluids **28**, 759 (1985); E. J. Hinch, in *Disorder and Mixing*, edited by E. Guyon, J.-P. Nadal, and Y. Pomeau (*Kluwer Academic*, Dordrecht, 1988), pp. 153–161; D. L. Koch, Phys. Fluids **6**, 2894 (1994); A. J. C. Ladd, Phys. Rev. Lett. **76**, 1392 (1996); Phys. Fluids **9**, 491 (1997).
[5] J. M. Ham and G. M. Homsy, Int. J. Multiph. Flow **14**, 533 (1988); H. Nicolai and E. Guazzelli, Phys. Fluids **7**, 3 (1995); H. Nicolai, B. Herzhaft, E. J. Hinch, L. Oger, and E. Guazzelli, Phys. Fluids **7**, 12 (1995); X. Lei, B. J. Ackerson, and P. Tong, Phys. Rev. Lett. **86**, 3300 (2001).
[6] P. N. Segre, F. Liu, P. Umbanhowar, and D. A. Weitz, Nature (London) **409**, 594 (2001); E. Guazzelli, Phys. Fluids **13**, 1537 (2001); F. Rouyer, D. Lhuillier, J. Martin, and D. Salin, Phys. Fluids **12**, 958 (2000).
[7] D. L. Koch and E. S. G. Shaqfeh, J. Fluid Mech. **224**, 275 (1991); A. Levine, S. Ramaswamy, E. Frey, and R. Bruinsma, Phys. Rev. Lett. **81**, 5944 (1998); P. Tong and B. J. Ackerson, Phys. Rev. E **58**, R6931 (1998).
[8] M. P. Brenner, Phys. Fluids **11**, 754 (1999).
[9] J. H. C. Luke, Phys. Fluids **12**, 1619 (2000).
[10] R. H. Davis and M. A. Hassen, J. Fluid Mech. **196**, 107 (1988); S. Lee, Y. Jang, C. Choi, and T. Lee, Phys. Fluids A **4**, 2601 (1992); J. Martin, N. Rakotomalala, and D. Salin, Phys. Fluids **6**, 3215 (1994); J. Martin, N. Rakotomalala, and D. Salin, Phys. Rev. Lett. **74**, 1347 (1995).
[11] B. J. Berne and R. Pecora, *Dynamic Light Scattering; with Applications to Chemistry, Biology and Physics* (Wiley, New York, 1976).
[12] L. Cipelletti and D. A. Weitz, Rev. Sci. Instrum. **70**, 3214 (1999).
[13] P. J. Mucha *et al.* (to be published).
[14] A. E. Boycott, Nature (London) **104**, 532 (1920).